

Controlling Metal Halide Perovskite Crystal Growth via Microcontact Printed Hydrophobic-Hydrophilic Templates

Zekarias Teklu Gebremichael,* Shahidul Alam, Nicola Cefarin, Alessandro Pozzato, Teketel Yohannes, Ulrich S. Schubert, Harald Hoppe, and Massimo Tormen*

Herein, a simple, low-cost, solution-processed, and parallel fabrication method to form metal halide perovskite (MHP) poly and single-crystalline films confined in ordered micrometer-sized domains is reported. A cross-linked polydimethylsiloxane (PDMS) stamp featuring 25 μm side squares is used to pattern their substrates. The substrate is microcontact printed on the PDMS inked with self-assembled monolayers (SAMs) of alkanethiol to form a molecular template, resulting in hydrophilic (gold) and hydrophobic (alkanethiol) domains. The subsequent deposition of lead bromide (PbBr_2) and methylammonium bromide (MABr) precursor solutions on the pre-patterned substrate resulted in poly and single-crystalline films of methylammonium lead bromide (MAPbBr_3) confined to the hydrophilic domains. Two deposition methods: drop-casting and two-step spin-coating are systematically investigated to find well confined and large-sized single-crystal MAPbBr_3 . Casting proves to be more effective than two-step spin-coating to achieve better confinement of MAPbBr_3 . The patterning process is monitored in dependence of the a) deposition methods used to b) precisely control the MAPbBr_3 crystal growth in a pre-defined site which leads to c) grow poly and single-crystals in a periodic arrangement. Their nondestructive and less energy processable fabrication method will have its own contribution in transferring patterns to desired substrates that enables them to fabricate different types of MHP optoelectronic devices and integrated electronic systems with more complex architectures.

1. Introduction

Metal halide perovskite (MHP), and in particular methylammonium lead halides, MAPbX_3 ($\text{MA} = \text{CH}_3\text{NH}_3$ and $\text{X} = \text{I}, \text{Br}, \text{Cl}$) show remarkable properties in photovoltaics and a wide range of optoelectronic applications such as photodetectors, lasers, high energy radiation detector, and light-emitting diodes (LEDs).^[1] Ten years after the first report of a hybrid metal halide perovskite solar cell (PSC), the power conversion efficiency (PCE) of a small device based on polycrystalline perovskite films has increased from 3.8%^[2] to a certified value of 25.5%.^[3] Following the progress of perovskite deposition methods, it is reported that patterning the perovskite film on a nanoscale or microplate can improve the performance of devices both in photovoltaics and optoelectronic fields.^[4] For instance, the performance of solar cells can be increased by patterning the film, which reduces surface reflectance, cutting light trapping, and directionality.^[4b]

Nowadays, several patterning methods have been developed by different groups to realize single-crystalline microplates

Z. T. Gebremichael, S. Alam, U. S. Schubert, H. Hoppe
Laboratory of Organic and Macromolecular Chemistry (IOMC)
Friedrich Schiller University Jena
Humboldtstr. 10, Jena 07743, Germany
E-mail: zekariasteklu.gebremichael@uni-jena.de

Z. T. Gebremichael, S. Alam, U. S. Schubert, H. Hoppe
Center for Energy and Environmental Chemistry Jena (CEEC Jena)
Friedrich Schiller University Jena
Philosophenweg 7a, Jena 07743, Germany

Z. T. Gebremichael, T. Yohannes
Department of Chemistry
Addis Ababa University
4 killo King George VI, Addis Ababa 1176, Ethiopia

Z. T. Gebremichael, M. Tormen
IOM-CNR
Area Science Park, Basovizza, S.S. 14, Km. 163.5, Trieste 34149, Italy
E-mail: massimo.tormen@thundernil.com

N. Cefarin
University of Trieste
Piazzale Europa, Trieste 134127, Italy
N. Cefarin, A. Pozzato, M. Tormen
ThunderNIL s.r.l. via Ugo Foscolo 8
Padova 35131, Italy

 The ORCID identification number(s) for the author(s) of this article can be found under <https://doi.org/10.1002/crat.202100121>

© 2021 The Authors. Crystal Research and Technology published by Wiley-VCH GmbH. This is an open access article under the terms of the Creative Commons Attribution-NonCommercial-NoDerivs License, which permits use and distribution in any medium, provided the original work is properly cited, the use is non-commercial and no modifications or adaptations are made.

DOI: 10.1002/crat.202100121

MHP fabrication. The earliest patterned distributed-feedback (DFB) of MHP reported by Jia et al.^[5] were fabricated by etching silicon substrate and coating the perovskite precursor. Gholipour et al.^[6] used focused ion beam (FIB) milling to pattern perovskite directly to build textures over a small area. Wang et al.^[1a] reported the first patterned growth of regular arrays of methylammonium lead iodide (MAPbI₃) perovskite microplate crystals for functional electronics and optoelectronics. They grew an array of MAPbI₃ single-crystals from the two-step deposition method directly on a photolithographically patterned silicon wafer substrate. However, patterning of perovskite in microplates scale on conventional charge transport layers has their own limitations. To overcome this limitation, Wu et al.^[7] report a wettability-assisted blade-coating process to pattern the perovskite precursor solution into arrays. On fluorine-doped tin oxide (FTO) substrate, they deposited, titanium dioxide (TiO₂), Poly(N,N'-bis-4-butylphenyl-N,N'-bisphenyl)benzidine (Poly-TPD), and photoresist layers, respectively. In subsequent steps, they patterned the poly-TPD layer and were able to produce patterned single-crystal methylammonium lead bromide (MAPbBr₃) perovskite on it.

In the patterning and structuring of MHP, a scalable and compatible technique is required that takes advantage of solution-based processing of the perovskite, which is more desirable. To this end, in our previous work, we have used nanoimprint lithography to pattern spin-coated perovskite films through heated and pressurized contact with inflexible stamp.^[8] On the other hand, Mao et al.^[9] fabricated a directly patterned nanostructure of MHP deposited from solution using flexible polydimethylsiloxane (PDMS) stamps. Unlike a silicon stamp, the PDMS can imprint its textures conformally on non-uniform surfaces and over defects.^[10] In this regard, the use of PDMS stamps in place of the master during patterning can save from the risk of damaging the expensive master. Up to 370 nm features have been imprinted into perovskite films using a PDMS stamp and a recrystallization process assisted by exposure to methylamine gas.^[9] Likewise, Park et al.^[11] reported patterned MAPbBr₃ and MAPbI₃ on different substrates such as silicon dioxide (SiO₂), gold (Au), indium tin oxide (ITO), FTO, and aluminium oxide (Al₂O₃) with periodic lines, squares, and hexagons. In their investigation, a perovskite solution was spin-coated on silicon substrate followed by co-frontal contact with prepatterned PDMS mold. The micropatterned precursor film in gel state on the PDMS mold was further transferred on a desired substrate giving rise to a micropatterned perovskite film on the substrate. Such patterning techniques, including our present work, are particularly appropriate for solution-processed MHP. This is because MHP's are very sensitive to water and plasma processing, making them incompatible with conventional lithography and etching processes.

In this direction, we were able to design a method of transferring the pattern on a silicon wafer, patterned using photolithography into a PDMS stamp. And then, the pattern created on the PDMS was successfully transferred into a purposely selected substrate (within 30 s), on which one can deposit and grow poly and single-crystalline perovskite films. Our present work successfully patterning MHP crystals (both polycrystalline and single-crystal) exploits a spatial modulation of wetting properties of the substrate. This may offer the ability to grow MHP crystals and precisely place them at specific positions of substrate that can be used for LED and high energy radiation detectors.^[1d,1e,12]

2. Experimental Section

2.1. Preparation of Methylammonium Bromide (MABr)

All the solvents and chemicals the authors have used in this research work were received from chemical providers more from Sigma Aldrich and used without further purification unless otherwise mentioned. These were dry Isopropanol, IPA (99.9%, Sigma-Aldrich), ethanol (99.8%, Sigma-Aldrich), dimethylformamide, DMF (anhydrous, 99.8%, Sigma-Aldrich), alkanethiol; C₁₆H₃₄-SH (99%, Sigma-Aldrich), lead bromide, PbBr₂ (99.99%, Sigma-Aldrich), hydrobromic acid, HBr (48% in water, Sigma-Aldrich), methylamine (33 wt-% in ethanol, Sigma-Aldrich). Methylammonium bromide (MABr) was synthesized according to the synthesis protocol of organic halide used as perovskite precursor materials reported in Ref. [13]. Methylamine (36.4 mL) and HBr (23.3 mL) were mixed into round bottom flask (250 mL). After continuous stirring at 0 °C for 2 h, the homogeneous transparent solution was evaporated using a rotavapor set up at 50 °C. The resulting pale yellow precipitate of MABr product was washed with mixed solvent of diethyl ether and ethanol, followed by filtration and drying at 60 °C in a vacuum oven for 24 h. The white MABr crystal obtained from this synthesis was used to prepare MAPbBr₃.

2.2. Preparation of Halide Perovskite Precursor Solutions

All the perovskite precursor solutions were prepared at room temperature in the air inside a cleanroom condition. Lead bromide, PbBr₂ was dissolved in DMF with a concentration of (1 M). The laboratory synthesized MABr (2 M) was separately dissolved in dry IPA for the two step deposition. For the drop cast deposition, two different concentration of (1 M) and (1.5 M) MAPbBr₃ solution were prepared by dissolving PbBr₂ and MABr (1:1 molar ration) in DMF solvent. All these freshly prepared perovskite precursor solutions were kept warm on a hot plate at 70 °C for 3 h under strong magnetic stirring during the experiments.

2.3. Preparation of the Silicon Mold

Photolithography is a well-established optical technology for transferring a pattern from a photomask to a photosensitive resin film deposited on the surface of a solid substrate such as a silicon wafer.^[14] The silicon master used for the PDMS stamps patterning, was fabricated by a combination of UV photolithography and reactive-ion etching. A photomask with a 35.6 μm period square array (chromium) of 25 μm side (corresponding to a filling factor of 0.5) was used to UV-expose a photoresist film on 4" silicon (100) substrate. Prior to photolithography, silicon substrate was degreased in ultrasonic baths of acetone, methanol, and deionized water for 2 to 5 min each and blown dry with a nitrogen stream. Hexamethyldisilazane (HMDS) was spin-coated as a surface adhesion promoter on the substrates at 2000 rpm for 30 s and baked at 115 °C for 60 s. Next, a positive AZ9260 photoresist was spin-coated at 2000 rpm for 30 s and soft-baked at 110 °C for 60 s, followed by UV exposure and the development of the photoresist in HF319 for 25 s. The pattern was transferred into the silicon

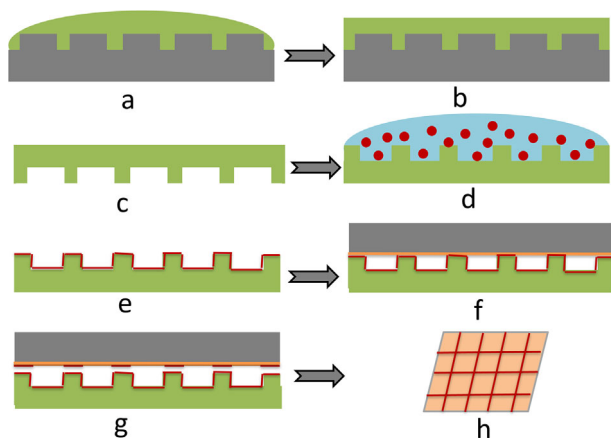


Figure 1. Cross-section scheme showing a) pouring of liquid PDMS onto patterned silicon wafer, b) PDMS baking, c) patterned PDMS stamp, d) PDMS stamp inked with alkanethiol molecules solution, e) SAM of thiols on PDMS stamp, f) microcontact printing of Si/Cr/Au substrate surface on thiol wetted PDMS stamp, g) selectively transferring a SAM of alkanethiol molecules on the substrate, and h) Si/Cr/Au substrate with hydrophilic-hydrophobic contrast ready for MAPbBr₃ confinement

wafer to a depth of 2 μm by reactive ion etching in an inductively coupled plasma system by a process at 8 mTorr pressure, C₄F₈, SF₆, and Ar flow of 60, 30, and 10 sccm, respectively, and 400 and 20 W radio-frequency powers applied to coil and platen, respectively.

2.4. Preparation of Polydimethylsiloxane (PDMS) Stamp

Two-component silicone elastomer solution was backed on top of the pre-patterned silicon wafer (mold) to prepare cross-linked polydimethylsiloxane (PDMS) stamp featuring 25 μm side squares. The authors have used a commercial PDMS material, Sylgard184 (Dow Corning) and was prepared according to the steps reported in Ref. [15], which those authors used for patterning MAPbBr₃. It is reported that cured PDMS has a very low surface energy and is inherently inert in character, making it free of contamination for chemical species to interact with its surface.^[16] **Figure 1a–c** depicts the steps followed in the PDMS stamp preparation. The viscous mixture of the monomer and curing agent 10:1 (w/w) Sylgard184 was casted on the cleaned mold (Figure 1a). After degassed in vacuum to remove air bubbles, it was thermally cured on a hot plate at 120 $^{\circ}\text{C}$ for 3 h (Figure 1b). The cross-linked elastomeric PDMS stamp featuring 25 μm side squares holes in a 35.4 μm period square array (corresponding to a filling factor of 0.5) was peeled off from the mold (Figure 1c). The low adhesion of the PDMS to the master allows the stamp to be peeled undamaged from the master, which is an exact negative replica of the master.^[16]

2.5. Microcontact Printed Self-Assembled Monolayer of Alkanethiol on Gold

Gold-coated silicon, 4" (100) wafer substrate with nominal resistivity of 10–100 Ωcm was used for the confinement of MAPbBr₃,

throughout this research work. The wafer was first cleaned from organic contaminants by oxygen plasma. Next, it was coated sequentially with a film of chromium and gold, Cr/Au (10/20 nm) using thermal evaporation machine and diced into 1.5 \times 1.5 cm² pieces of silicon/chromium/gold (Si/Cr/Au) substrates for the experiments. Because gold has lower surface adhesion as compared to chromium, 10 nm chromium was evaporated to enhance the deposition of gold. Before the microcontact printing step, the PDMS has to be inked with alkanethiols. Alkanethiol molecules self-assemble (SAM) on noble-metal surfaces such as gold, silver and copper (Au, Ag, and Cu) to form dense, ordered monolayers.^[16] Initial assembly occurred in a matter of seconds, both from solution and from elastomeric stamps.^[14] By using alkanethiols of different chain lengths, the surface energy of SAM could be controlled.^[17] Because of the partial depletion of alkanethiols from PDMS stamp, inking of the PDMS stamp needed to be done in every three micro-contact printing processes. In the present work the authors use (5 mM) of alkanethiol (C₁₆H₃₄-SH) solution in ethanol to ink their PDMS stamp.

Usually, microcontact printing consists of two main steps, that is, the transfer of a SAM from a patterned elastomeric membrane onto the surface of a noble metal or a wet etching step that exploits the protective characteristics of the SAM to etch only the unprotected areas of the noble metal.^[16] The patterned side of PDMS stamp was inked by the alkanethiol solution (Figure 1d), and blown dry after 10 s under nitrogen stream (Figure 1e). The Si/Cr/Au substrate is then contacted on the thiol wetted PDMS stamp for 25 to 30 s (Figure 1f), selectively transferring SAM alkanethiol molecules on gold and forming a pattern corresponding to the protruding features on the stamp (Figure 1g). The authors successfully transferred the pattern on PDMS to another substrate rather than using the PDMS itself for patterning an MHP film directly on it.^[9] The MHP precursor solution will then be deposited from the solution on both of the hydrophilic-hydrophobic contrast surfaces of the substrate shown in Figure 1h. The SAM thiols will evaporate during the annealing step of the perovskite film.

3. Characterization

The patterned structure of both silicon mold and PDMS stamp were checked using a microscope setup integrated with a computer monitor by which one can see clearly an array of the patterns. The microscopic photos showing confinement of MAPbBr₃ crystal film were also taken from a microscopic view of the substrate after deposition of the MAPbBr₃ perovskite. The surface morphology of MAPbBr₃ films were analyzed by using a ZEISS FEGSEM Supra 40 Scanning Electron Microscope, SEM (Carl-Zeiss AG, Germany) operating at 5 kV accelerating voltages. And to analyze the elemental composition of MAPbBr₃ single crystals fabricated using the two-step deposition method, we use an Oxford energy dispersive spectroscopy (EDS) system in combination with a Sigma VP Field Emission SEM performed with a 50 mm² XMax detector. The photolithographic patterning of silicon wafer (mold) was performed on a SUSS MA6 mask aligner. The steady-state photoluminescence (PL) spectra was recorded with an Avantes AvaSpec ULS-2048 fiber spectrometer with a laser diode emitting at 405 nm. And the calculated absorbance

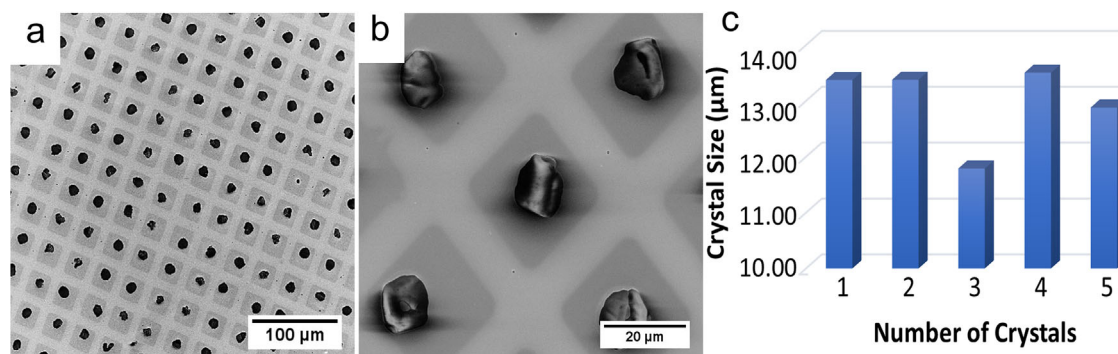


Figure 2. Top-view SEM image of confined MAPbBr₃ single crystals fabricated using two-step spin-coating deposition method a) at scale bar of 100 μm, b) scale bar of 20 μm, and c) histogram, showing single crystals size distribution.

was recorded with two Avantes AvaSpec-ULS3648- USB2-UA-25 fiber spectrometers.

4. Results and Discussion

4.1. Confinement of Methylammonium Lead Bromide (MAPbBr₃) Perovskite

The aim of this research work is to find suitable conditions to pattern MAPbBr₃ poly- or single-crystals in an array of periodic arrangement of targeted sites. MAPbBr₃ perovskite was selected for its tendency to form large crystals up to a macroscopic size and its bandgap (≈ 2.2 eV) suitable for light-emission applications such as lasing and LED.^[1b,18] We investigated the fabrication of patterned MAPbBr₃ crystals by exploiting the surface energy contrast between bare gold and gold with micro-contact printed on SAMs of alkanethiol wetted PDMS stamp using two deposition methods, that is, spin coating and drop-casting. During spin-coating, the perovskite material migrates and deposits selectively on the hydrophilic part (gold), and de-wetting from regions of low surface energy (hydrophobic).^[14] We demonstrate the effectiveness of this approach by fabricating patterned poly and single-crystalline aggregates of MAPbBr₃.

4.1.1. Two-Step Spin-Coating Deposition of Perovskite Precursors

The authors used the two-step sequential deposition method developed by Burschka et al.^[19] to confine and grow MAPbBr₃ perovskite crystals. This kind of deposition method is commonly used to fabricate polycrystalline perovskite thin films. The Si/Cr/Au substrate was microcontact printed by gently contacting on (5 mm) of C₁₆H₃₄-SH thiol inked PDMS stamp for 30 s. Next, PbBr₂ solution (1 M) was spin-coated onto the substrate at 2000 rpm for 30 s and annealed for 3 min at 100 °C. After a short interval, MABr solution (2 M) was spin-coated at 1000 rpm for 30 s, followed by annealing the final layer stack film at 100 °C for 15 min. This process led to the deposition and growth of MAPbBr₃ perovskite crystalline material confined in each hydrophilic square domain, de-wets from the hydrophobic regions of the substrate during spin-coating. The morphology

of the perovskite observed by SEM and optical microscopy appeared to be almost unaffected by the annealing conditions and consisted mostly of single-crystals of MAPbBr₃ perovskite in every hydrophilic square of the substrate. However, as shown in **Figure 2**, the crystals are not filling the entire hydrophilic square areas. In order to show the crystal size distribution among the patterned perovskite single-crystal prepared by this method, we have chosen the SEM images in **Figure 2b**. The size of patterned single-crystals is very close to each other and ranges from 11.789 to 13.504 μm, as shown in the histogram (**Figure 2c**) calculated using ImageJ.

The elemental composition of the resulted single-crystal and the conversion of PbBr₂ and MABr into MAPbBr₃ made from the sequential deposition was analyzed using EDS measurement maps. As can be seen from the EDS image in **Figure 3b,c**, the lead and bromine ions are incorporated in the MAPbBr₃ perovskite micro-scale-single crystal shown in **Figure 3a**. A thin layer of MAPbBr₃ nano-sized clusters appearing as darker square areas surrounding the crystals (**Figure 2**) above covers entirely the hydrophilic squares of the array. This is confirmed by the EDS images that show highly correlated Pb and Br signals not only in the region of the micro-crystal but also on the surrounding nanoscale clusters (**Figures 3b and c**).

4.1.2. Drop Casting Deposition of Perovskite Precursor

In this casting method, the hot MAPbBr₃ (1 M) precursor solution was drop casted on the microcontact printed substrate. After 5 min loading time, the excess solution was shaken off from the substrate and annealed at 70 °C for 60 min. Complete coverage of the hydrophilic squares with a poly-crystalline (collection of nano/micro-sized crystals) of MAPbBr₃ film was obtained, as confirmed from the micrograph (**Figure 4a**) and SEM image (**Figure 4b,c**). Casting proved to be more effective than two-step spin-coating to achieve perovskite confinement but was unable to produce MAPbBr₃ single-crystals. This can be stemmed from the longer annealing time that limits the recrystallization of the perovskite.^[15] Attempts were made to re-crystallize the film into larger MAPbBr₃ micro-crystals by overnight room temperature solvent annealing in DMF vapor through Ostwald ripening process.^[20] According to the theory of Ostwald ripening, smaller crystals would dissolve and redeposit onto the more giant crystal.

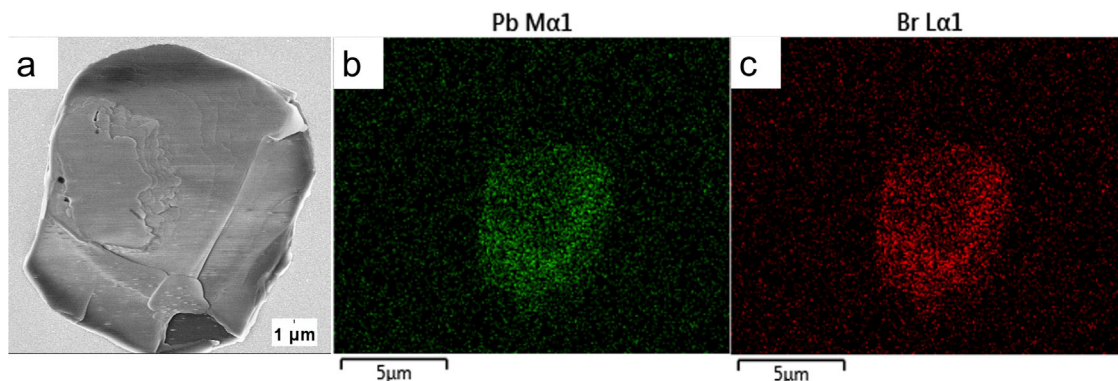


Figure 3. Energy dispersive spectroscopy (EDS) images showing a) SEM image of MAPbBr₃ single crystal, b) Pb content, and c) Br content in MAPbBr₃ single crystal fabricated using two-step spin coating method .

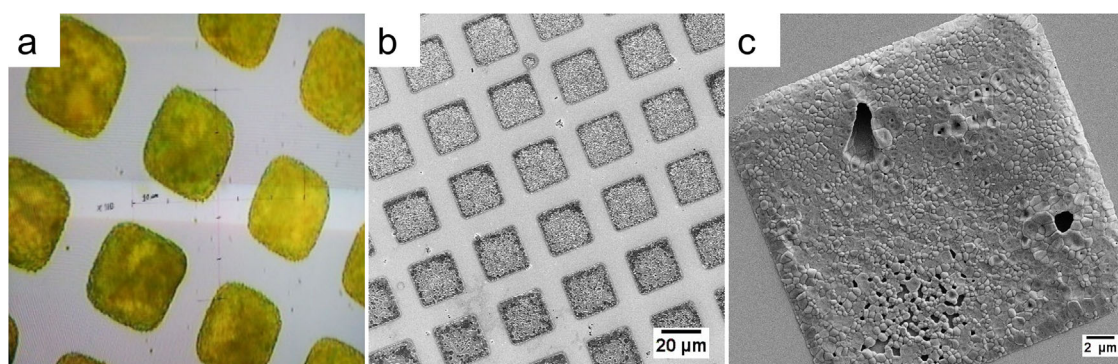


Figure 4. Confined MAPbBr₃ poly-crystalline in a square arrays of a) optical micrograph photo, b) top view SEM image and c) tilted SEM image in one square site.

However, it was not possible to identify suitable conditions that could lead to a significant increase in crystal size. But, in a similar patterning of perovskite deposited by blade coating method, Wu et al.^[7] were successful in growing microplate MAPbBr₃ single-crystals by employing IPA and DMF solvents assisted recrystallization process with careful control of the amount of DMF solvent. In our case, the already formed nano-crystals did not provide the conditions for them to recrystallize into larger crystals and the structures remains frozen in the polycrystalline structure.

Motivated by the fact that the drop-casting method resulted in complete coverage of the hydrophilic square areas, we modified the deposition process. Instead of shaking off the solution from the substrate after 5 min loading time and annealing the residual wet layer for a longer time, the drop-casted solution was simply kept on the substrate during the annealing step for a shorter time. For this experiment, a hot MAPbBr₃ precursor solution (1.5 M) was cast onto the patterned substrate covering its entire surface. The substrate, kept in a petri dish, was immediately placed on a hot plate at 70 °C and annealed for 3 min. Removing from the hot plate, the solution was shaken off gently from the substrate and allowed to dry spontaneously at room temperature. **Figure 5** shows the optical micrograph photo and SEM images at different magnifications of patterned aggregates of single-crystals of MAPbBr₃ perovskite. We observe that the hydrophobic area of the substrate surface provides effective boundaries to the growth

of the crystals. In fact, crystal appears to grow up to the edges of hydrophilic areas (Figure 5b) without significant over-growing into the hydrophobic areas.

With regard to the confined perovskite crystal size growth, the result in Figure 5 proved to be better than that of the result in Figure 4. In Figure 5, the substrate was annealed before removing the solution from it. In contrast, in the first case, the substrate was annealed after the solution is removed irrespective of the annealing time variation in between. We have tried to repeat the promising result shown in Figure 5 with an additional drying step at 70 °C for 1 min. This is to elucidate how to instate post-annealing after the removal of solution will affect the crystal growth nature of MAPbBr₃. The hot MAPbBr₃ solution was over casted on the patterned substrate. As revealed from **Figure 6**, even if the confinement is still working, but the idea of growing only a single-crystal perovskite is still challenging to manage. And hence we are still with more than one single-crystal in almost all confined materials. On top of this, the additional drying step at 70 °C for 1 min together with the spontaneous drying of the sample, may contribute in changing the morphology of MAPbBr₃ perovskite crystallinity as compared to what is obtained in Figure 5. It seems that the drop cast deposition method shows the possibility to grow large sized single-crystals of perovskite in every site of the patterned substrate of the processing parameters, for example, the nucleation time, casting method, drying time, and annealing temperature, are well controlled. This can be witnessed by

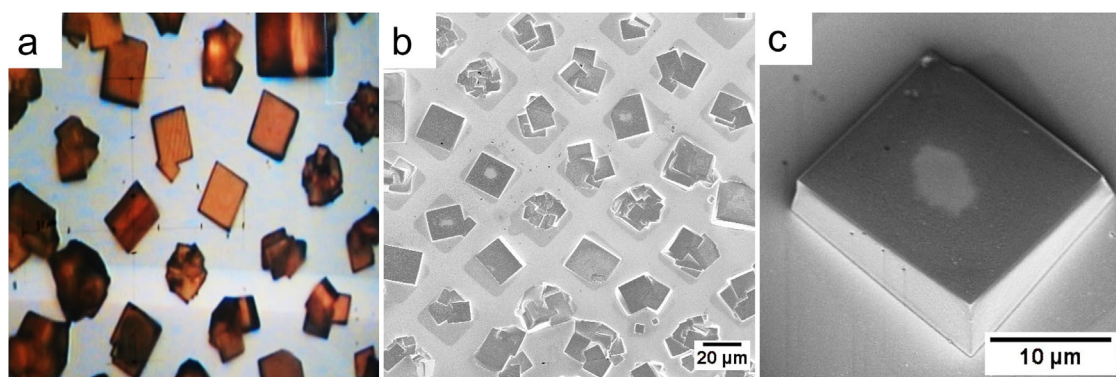


Figure 5. Confined MAPbBr₃ single crystals in a square arrays of a) optical micrograph photo, b) top view SEM image and c) tilted SEM image of single-crystal in one square site.

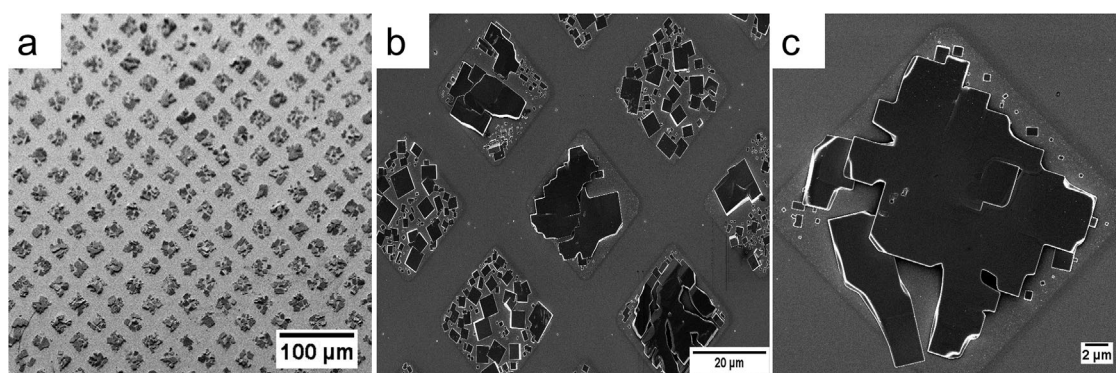


Figure 6. Top view SEM images of confined MAPbBr₃ single crystals in a square arrays at a) 100 μm b) 20 μm and c) 2 μm scale bares

looking at Figure 6c how the neighboring single-crystals confined in one site are joining and coming up to grow into single-crystal and almost filling the $25 \times 25 \mu\text{m}^2$ pattern square area. However, further investigation needs to be done in this regard.

In order to know the effect of annealing temperature, annealing time, and perovskite solution concentration on the crystallization process, we have investigated the same deposition process for the drop-casting method on unpatterned substrates. The effect of annealing before and after removing the solution (ABRS and AARS) was also investigated. Annealing the substrate at 70 °C for a short time with the solution on its surface, induces the crystal to evolve into a larger crystal size domain (Figure 7a). This is maybe due to the simultaneous solvent annealing effect^[21] and more material on top. Whereas the annealing steps after removing the solution resulted in small size crystal growth (Figure 7b). Annealing time at 70 °C was set to 1, 3, 5, and 10 min. As it can be noticed from the SEM images in Figures 7c,d,f and/or 7g–i, for the solution on top, the annealing time has no considerable effect on the crystallinity of perovskite. In particular, after 3 min annealing time, almost the same size crystal domains are obtained. However, for the same procedure and the same annealing time of 3 min, changing the concentration from (1.0 to 1.5 M) contributes to the increment of the MAPbBr₃ perovskite crystal size growth (Figure 7a,d). That is why the crystal size displayed in Figure 5 is larger than that in Figure 4.

All the simple and manageable methods and results obtained in this study can contribute to directly grow MHP crystals onto pre-patterned substrates to form functional devices as in the literature.^[22] With this approach, large arrays of independently addressable devices may be easily prepared by selective nucleation and growth of poly- and or single-perovskite crystals between arrays of electrode pairs.^[1a] Both the two deposition methods we have used (two-step spin coating and drop-casting) are adequate to confine the MHP in the desired squares site of the pre-patterned substrate. The two-step spin coating method is resulted in almost all single crystal (as checked by SEM) of MAPbBr₃ confined in every square site of the substrate. The short outcome of this method is, the crystals are small in size (with an average crystal size of 12.5 μm). In the drop-casting method, the annealing step at 70 °C with the solution on top helps the crystal to evolve into a larger crystal size domain due to the simultaneous solvent annealing effect and MAPbBr₃ solubility property.

Evidence of optical characterization of the final material system (patterned MAPbBr₃) is important to prove its possibility in optoelectronic applications. We have included here the absorbance and photoluminescence (PL) characteristics of the MAPbBr₃ films deposited and growth by two-step spin coating and drop casting methods on glass substrate. As it can be seen from Figure 8a, the MAPbBr₃ crystal obtained from the two-step spin coating method has a sharp absorbance onset, indicating characteristic single crystals of MAPbBr₃, which is

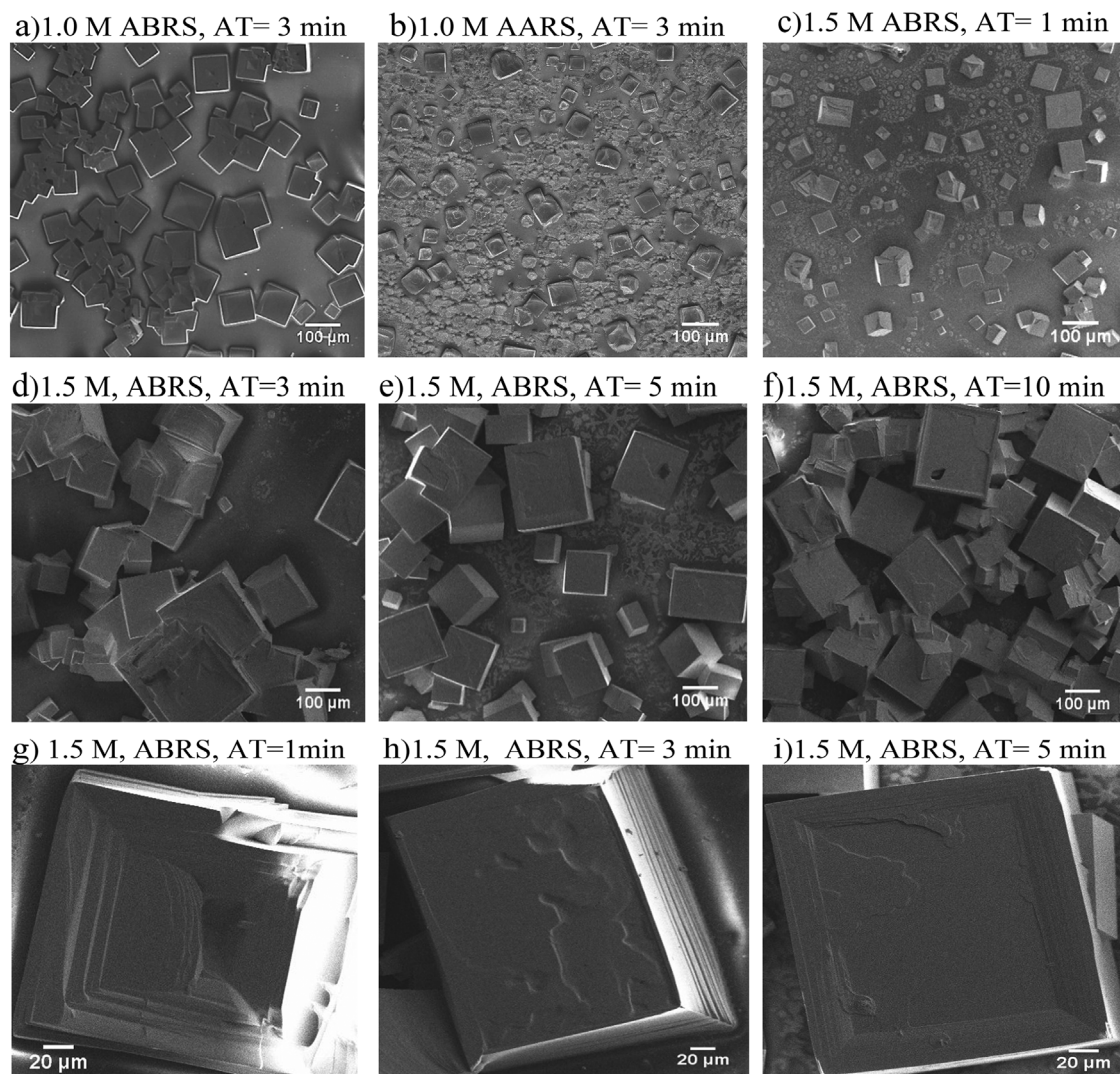


Figure 7. Top-view SEM images with different scale bars, a) 1.0 m MAPbBr₃ film annealed before removing MAPbBr₃ solution (ABRS) from the substrate for annealing time 3 min, b) 1.0 m MAPbBr₃ film annealed after removing MAPbBr₃ solution (AARS) from the substrate for annealing time 3 min, c–f) poly-crystalline and g–i) single crystals of 1.5 m MAPbBr₃ film annealed before removing MAPbBr₃ solution from the substrate for annealing time 1, 3, 5, and 10 min, respectively.

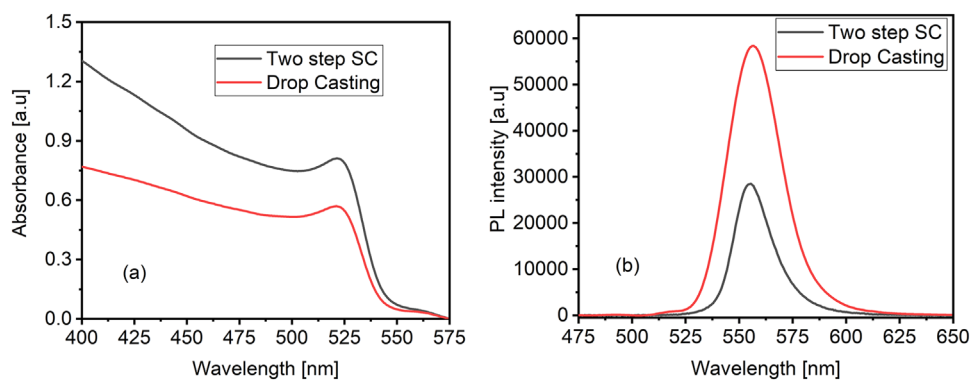


Figure 8. a) Absorbance and b) photoluminescence of MAPbBr₃ films deposited from (1 m) MAPbBr₃ by two-step spin coating and drop casting methods.

also confirmed from the SEM images (Figure 2) and narrow and sharp PL peak (Figure 8b). A single crystal of MHP (particularly MAPbI₃ and MAPbBr₃) are characterized by sharp absorbance onset and narrow PL peak as compared to their poly-crystalline counter parts.^[23] These optical characteristics are also confirming the formation of MAPbBr₃ from both deposition methods used which are in consistence with the SEM images of MAPbBr₃ crystals.

5. Conclusion

We demonstrate that the hydrophobic–hydrophilic contrast created on the substrate using SAM thiols wetted PDMS stamp is very effective to grow perovskite crystals confined in periodic arrangements. Even though the total surface of substrate was covered by perovskite precursor solution during deposition (by spin coating and drop casting), we observe that the hydrophobic area of the substrate surface provides effective boundaries to the growth of the perovskite crystals only in the hydrophilic domain. We are successful in transferring the pattern from silicon wafer to PDMS stamp and to another suitable solid substrate within 30 s, on which we were able to confine and grow MAPbBr₃ perovskite materials ranging from aggregated, polycrystalline film, and single-crystals of different sizes. In addition to controlling crystal growth and confinement of MAPbBr₃, the dimensionality and crystallographic orientation of the perovskite crystals growth are in alignment with the dimension of the patterned area of the substrate. The two-step deposition method tends to be the best confinement to obtain only single-crystal of MAPbBr₃, as compared to the drop cast deposition method resulting in the aggregation of single-crystals confined in one site. Of the later method, the annealing step with precursor solution on top of the substrate provides better perovskite crystallinity. The entire process of perovskite crystal growth and film fabrication occurs at a rather low temperature (<70 °C). Further investigations need to be done in the direction of optical characterizations, optimizing the concentration and deposition steps to have better confinement in the way to produce only single-crystal perovskite with desired sizes that can be used for a semiconductor material system as light emitting diodes and high energy radiation detectors.

Acknowledgements

Z.T. acknowledges the financial support of ICTP under the framework of ICTP-TRIL (Training and Research in Italian Laboratories) fellowship programme (Ref.2353) and DAAD scholarship (Funding programme/-ID: 57299294). The authors are grateful to IOM-CNR for giving the access to laboratories and microfabrication equipment. The authors appreciate for some of the SEM measurements support by Steffi Stumpf at IOMC, Jena, Germany.

Open access funding enabled and organized by Projekt DEAL.

Conflict of Interest

The authors declare no conflict of interest.

Data Availability Statement

The data that support the findings of this study are available from the corresponding author upon reasonable request.

Keywords

confinement, methylammonium lead bromide (MAPbBr₃), microcontact imprinting, photolithography, polydimethylsiloxane (PDMS), silicon wafer

Received: June 14, 2021

Revised: August 30, 2021

Published online: October 20, 2021

- [1] a) G. M. Wang, D. H. Li, H. C. Cheng, Y. J. Li, C. Y. Chen, A. X. Yin, Z. P. Zhao, Z. Y. Lin, H. Wu, Q. Y. He, M. N. Ding, Y. Liu, Y. Huang, X. F. Duan, *Sci. Adv.* **2015**, *1*; b) K.-H. Wang, L.-C. Li, M. Shellaiah, K. W. Sun, *Sci. Rep.* **2017**, *7*, 13643; c) D. W. deQuilettes, S. M. Vorpahl, S. D. Stranks, H. Nagaoka, G. E. Eperon, M. E. Ziffer, H. J. Snaith, D. S. Ginger, *Sci.* **2015**, *348*, 683; d) W. Y. Nie, H. H. Tsai, R. Asadpour, J. C. Blancon, A. J. Neukirch, G. Gupta, J. J. Crochet, M. Chhowalla, S. Tretiak, M. A. Alam, H. L. Wang, A. D. Mohite, *Sci.* **2015**, *347*, 522; e) C. C. Stoumpos, C. D. Malliakas, J. A. Peters, Z. F. Liu, M. Sebastian, J. Im, T. C. Chasapis, A. C. Wibowo, D. Y. Chung, A. J. Freeman, B. W. Wessels, M. G. Kanatzidis, *Cryst. Growth Des.* **2013**, *13*, 2722.
- [2] K. T. Akihiro Kojima, Y. Shirai, T. Miyasaka, *J. Am. Chem. Soc.* **2009**, *131*, 6050.
- [3] Best Research-Cell Efficiency Chart, <https://www.nrel.gov/pv/cell-efficiency.html>
- [4] a) M. L. Brongersma, Y. Cui, S. Fan, *Nat. Mater.* **2014**, *13*, 451; b) Y. Cui, D. Van Dam, S. A. Mann, N. Van Hoof, P. Van Veldhoven, E. Garnett, E. Bakkers, J. Haverkort, *Nano Lett.* **2016**, *16*, 6467.
- [5] Y. Jia, R. A. Kerner, A. J. Grede, A. N. Brigeman, B. P. Rand, N. C. Giabink, *Nano Lett.* **2016**, *16*, 4624.
- [6] B. Gholipour, G. Adamo, D. Cortecchia, H. N. Krishnamoorthy, M. D. Birowosuto, N. I. Zheludev, C. Soci, *Adv. Mater.* **2017**, *29*, 1604268.
- [7] J. Wu, F. J. Ye, W. Q. Yang, Z. J. Xu, D. Y. Luo, R. Su, Y. F. Zhang, R. Zhu, Q. H. Gong, *Chem. Mater.* **2018**, *30*, 4590.
- [8] N. Cefarin, A. Cian, A. Sonato, E. Governigo, F. Suran, Z. Teklu, A. Zanut, A. Pozzato, M. Tormen, *Microelectron. Eng.* **2017**, *176*, 106.
- [9] J. Mao, W. E. Sha, H. Zhang, X. Ren, J. Zhuang, V. A. Roy, K. S. Wong, W. C. Choy, *Adv. Funct. Mater.* **2017**, *27*, 1606525.
- [10] M.A. Verschuuren, Dissertation: Substrate Conformal Imprint Lithography for Nanophotonics, Utrecht University, 2010.
- [11] B. Jeong, I. Hwang, S. H. Cho, E. H. Kim, S. Cha, J. Lee, H. S. Kang, S. M. Cho, H. Choi, C. Park, *ACS Nano* **2016**, *10*, 9026.
- [12] a) H. J. Snaith, *J. Phys. Chem. Lett.* **2013**, *4*, 3623; b) D. Trimbach, K. Feldman, N. D. Spencer, D. J. Broer, C. W. M. Bastiaansen, *Langmuir* **2003**, *19*, 10957; c) W. Q. Liao, Y. Zhang, C. L. Hu, J. G. Mao, H. Y. Ye, P. F. Li, S. P. D. Huang, R. G. Xiong, *Nat. Commun.* **2015**, *6*, 7338; d) Q. Dong, Y. Fang, Y. Shao, P. Mulligan, J. Qiu, L. Cao, J. Huang, *Science* **2015**, *347*, 967; e) S. Li, C. Zhang, J. J. Song, X. Xie, J. Q. Meng, S. Xu, *Crystals* **2018**, *8*, 220.
- [13] S. Brittman, E. C. Garnett, *J. Phys. Chem. C* **2015**, *120*, 616.
- [14] Y. Xia, D. Qin, Y. Yin, *Curr. Opin. Colloid Interface Sci.* **2001**, *6*, 54.
- [15] S. Brittman, S. Z. Oener, K. Guo, H. Åboliņš, A. F. Koenderink, E. C. Garnett, *J. Mater. Chem. C* **2017**, *5*, 8301.
- [16] T. Kaufmann, B. J. Ravoo, *Polym. Chem.* **2010**, *1*, 371.
- [17] J. P. Folkers, P. E. Laibinis, G. M. Whitesides, *Langmuir* **1992**, *8*, 1330.
- [18] J. S. Huang, Y. C. Shao, Q. F. Dong, *J. Phys. Chem. Lett.* **2015**, *6*, 3218.
- [19] J. Burschka, N. Pellet, S.-J. Moon, R. Humphry-Baker, P. Gao, M. K. Nazeeruddin, M. Grätzel, *Nature* **2013**, *499*, 316.

- [20] M. Yang, T. Zhang, P. Schulz, Z. Li, G. Li, D. H. Kim, N. Guo, J. J. Berry, K. Zhu, Y. Zhao, *Nat. Commun.* **2016**, *7*, 12305.
- [21] Z. Xiao, Q. Dong, C. Bi, Y. Shao, Y. Yuan, J. Huang, *Adv. Mater.* **2014**, *26*, 6503.
- [22] a) Z. L. Chen, Q. F. Dong, Y. Liu, C. X. Bao, Y. J. Fang, Y. Lin, S. Tang, Q. Wang, X. Xiao, Y. Bai, Y. H. Deng, J. S. Huang, *Nat. Commun.* **2017**, *8*, 1890; b) N. L. Jeon, I. S. Choi, G. M. Whitesides, N. Y. Kim, P. E. Laibinis, Y. Harada, K. R. Finnie, G. S. Girolami, R. G. Nuzzo, *Appl. Phys. Lett.* **1999**, *75*, 4201; c) C. R. Kagan, T. L. Breen, L. L. Kosbar, *Appl. Phys. Lett.* **2001**, *79*, 3536; Mitzi David B., *J. Chem. Soc., Dalton Trans.* **2001**, *1*. <https://doi.org/10.1039/b007070j>; e) Z. Y. Cheng, J. Lin, *CrystEngComm* **2010**, *12*, 2646.
- [23] B. S. Swain, J. Lee, *Phys. E: Low-dimens. Syst. Nanostruct.* **2021**, *126*, 114420.